Effect of Winding Speed on the Structure and Properties of As-Spun Poly(trimethylene 2,6-naphthalenedicarboxylate) Fibers as Compared to Poly(ethylene terephthalate) Fibers

U. STIER, W. OPPERMANN

Institute for Man-Made Fibers; Körschtalstrasse 26, 73770 Denkendorf, Germany

Received 20 August 2001; accepted 6 October 2001

ABSTRACT: We present a comparative study of melt spinning of poly(trimethylene 2,6-naphthalenedicarboxylate) (PTN) and poly(ethylene terephthalate) (PET) fibers with respect to the effect of winding speed (2000–6000 m/min): Structural changes were followed by X-ray analysis, calorimetry, and measurements of density, boiling water shrinkage, and birefringence. As-spun PTN fibers exhibited a low degree of crystallinity at relatively low speeds (< 2000 m/min). An increase in winding speed up to 6000 m/min only resulted in a minor enhancement of crystallinity and orientation. The small change of structural parameters accounted for the fact that tenacity and modulus did not rise significantly with increasing winding speed, contrary to the PET fibers. © 2002 Wiley Periodicals, Inc. J Appl Polym Sci 84: 2489–2497, 2002

Key words: poly(trimethylene 2,6-naphthalenedicarboxylate) fibers; melt spinning; structure–property relation; crystallinity; orientation

INTRODUCTION

For thermoplastic polymers, such as polyesters, melt spinning is the most useful method for producing synthetic fibers. The development of crystallinity, molecular orientation, and the morphological features of fibers has generated great interest in fundamental research concerned with their mechanical and textile properties. In particular, intensive research has been done on poly(ethylene terephthalate) (PET) fibers with respect to the effect of winding speed on its structure and properties.[1–9]

Besides the commercially available terephtalates such as PET, poly(butylene terephthalate), and the recently introduced poly(trimethylene terephthalate) (PTT), a new group of polyesters based on naphthalates have become more and more important with poly(ethylene 2,6-naphthalenedicarboxylate) (PEN) as the best known. PEN exhibits thermal, mechanical, and barrier properties generally superior to those of PET, positioning PEN as a high-performance extension of PET with growing commercial importance.[10–12] The next homolog in the series of naphthalates, poly(trimethylene 2,6-naphthalenedicarboxylate) (PTN), however, has received only a little attention[13–16] (see Fig. 1).

Tsai and Lee[16] showed by differential scanning calorimetry (DSC) that the melting point and glass-transition temperature of PTN are 204 and 83°C, respectively. Our group recently studied the synthesis[17,18] and rheological properties[19] of PTN in detail. In this article, we focus on a systematic study of fibers to explore the structure–property relationship in the dependence of winding speed. The results are compared with PET fibers spun under the same set of process conditions.

Correspondence to: W. Oppermann (wilhelm.oppermann@itc.itvd.uni-stuttgartde).

Journal of Applied Polymer Science, Vol. 84, 2489–2497 (2002)

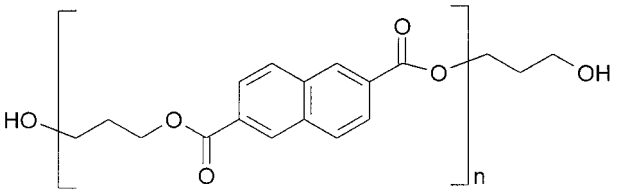

Figure 1 Structure of PTN.

In comparison to PET fibers, the naphthalene moiety in a PTN fiber should provide more stiffness to the linear backbone as shown for PEN.[10] On the other hand, the incorporation of 1,3-propanediol should lead to more flexibility according to the high resilience observed in PTT fibers.[20–24] Due to these contrary effects, it is very difficult to predict the structure–property relationship of PTN. Therefore, we carried out investigations to study the structural changes in the dependence of winding speed by means of X-ray analysis and calorimetry and measurements of density, boiling water shrinkage, and birefringence. The structural results are discussed with respect to the mechanical properties observed.

EXPERIMENTAL

Materials

A 20-L standard polycondensation autoclave (Fourné, Bonn) was used to produce PTN. The autoclave was fitted with a stirrer that comprised a torque measurement unit. A mixture of 8793 g (36 mol) of dimethyl 2,6-naphthalenedicarboxylate (2,6-DMN; Amoco, fiber grade) and 6849 g (90 mol) of 1,3-propanediol (Degussa, fiber grade) with 4.9 g (1.44×10^{-2} mol) of Ti(IV)butylate as a transesterification and polycondensation catalyst and 32 mg (1.44×10^{-4} mol) of triethyl phosphonoacetate as a stabilizer was placed in the reaction vessel. The transesterification reaction was carried out with stirring under a nitrogen atmosphere at 220°C, while the methanol was removed by distillation. When the transesterification was finished, the pressure was gradually reduced to 10 mbar. At the same time, the temperature was increased to a polycondensation temperature of 260°C. After the bulk of the 1,3-propanediol was removed, the pressure was further reduced to 10^{-1} mbar. The progress of polycondensation was controlled by the measurement of torque. When the torque reached a defined value, the reaction was stopped by a return to atmospheric pressure with nitrogen. The polymer melt was extruded with a spinning pump, cooled in an ice bath, and granulated. The relative solution viscosity of the PTN polymer was 1.88, measured as a solution of 1 g PTN in 100 mL of phenol/1,1,2,2-tetrachloroethane (1:1 w/w) at 20°C.

PET granulate Type 20 supplied by Hoechst AG was employed for the comparative study of the melt spinning of PTN and PET fibers.

Melt Spinning

Prior to the melt spinning, PTN granulate was dried at 130°C for 12 h under vacuum. PET granulate was dried at 160°C for 12 h. The melt spinning of PTN was carried out at wind-up speeds between 2000 and 6000 m/min in steps of 500 m/min at a temperature of 250°C (285°C for PET). The fibers were extruded from a 32 circular hole spinneret with a capillary diameter of 360 μm. The polymer throughput was adjusted in conjunction with the wind-up speed to achieve a comparable yarn fineness of approximately 120 dtex. The polymer extruded was taken up by a winder (SW 66 SSD, Barmag)

Density Measurements

The density of the samples was determined in a gradient column containing tetrachloromethane and *n*-heptane. The column with a linear density gradient was maintained at a constant temperature of 23°C.

Calorimetric Analysis

Calorimetric measurements were carried out with a PerkinElmer DSC 7 differential scanning calorimeter. Approximately 5 mg of the fiber sample was heated at a rate of 10°C/min under a nitrogen atmosphere.

Wide-Angle X-Ray Scattering (WAXS)

WAXS analyses were performed with nickel-filtered CuKα radiation (λ = 0.154 nm). We prepared the samples by winding a smooth layer of filaments around a metal frame. For the WAXS pattern, a texture goniometer (PW 1820, Philips) was employed.

Birefringence

Birefringence measurements were performed with a Leitz Laborlux 12 Pol polarizing micro-

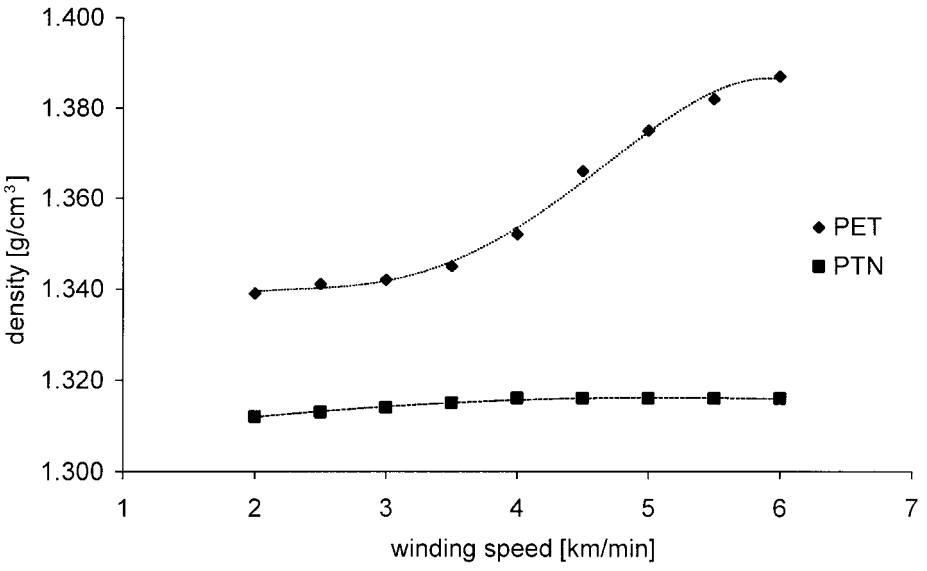

Figure 2 Density as a function of winding speed for PET and PTN fibers.

scope equipped with a Leitz compensator and a filter with $\lambda = 546$ nm. The filaments were positioned in parallel between microscopic glasses and placed at an angle of 45° relative to the crossed polarizers. The overall difference of phase δ was determined by measurement of the number of fringes. With help of an eyepiece micrometer, the diameter d of the filaments was measured. The birefringence (Δn) was calculated by means of the following formula:

$$\Delta n = \frac{\delta \cdot \lambda}{2\pi \cdot d}$$

Boiling Water Shrinkage

A loop of filaments whose initial length (l_0) was 49.5 cm under a slight tension that did not cause deformation, was immersed in boiling water for 30 min. The length after shrinkage (l_s) was measured under the same tension. Percentage shrinkage was determined with the following equation:

$$\text{Percentage Shrinkage (\%)} = \frac{l_0 - l_s}{l_0} \cdot 100$$

Tensile Measurements

Tensile tests were done on an automatic Textechno Statimat M according to DIN 53816. A gauge length of 200 mm and a constant crosshead speed of 200 mm/min were used. The load-elongation experiments were carried out 25 times for each fiber type, and the average was calculated.

RESULTS AND DISCUSSION

Density and Birefringence

Figures 2 and 3 show the density (a measure of crystallinity) and birefringence (a measure of molecular orientation) as a function of winding speed for as-spun PET and PTN fibers. Above a critical wind-up speed of approximately 3500 m/min, where the birefringence reached values of 0.06 or higher, the PET fiber crystallized in the spin line. This led to a steep increase in density. At highest winding speeds, a tendency toward saturation was observed. In contrast, the birefringence and density of the PTN fibers remained essentially constant over all winding speeds. Obviously, the use of higher speeds did not induce significant structural development in the PTN fiber.

As neither the density of fully amorphous and crystalline PTN is known nor is the birefringence of perfectly oriented crystalline and amorphous PTN, absolute values for crystallinity and orientation could not be calculated. To obtain some reference points, we quenched a PTN melt into ice water and determined the density of the sample to be $\rho_a = 1.305$ g/cm^{-3}. This should be the density of a nearly amorphous PTN because the thermally induced crystallization of PTN is very slow

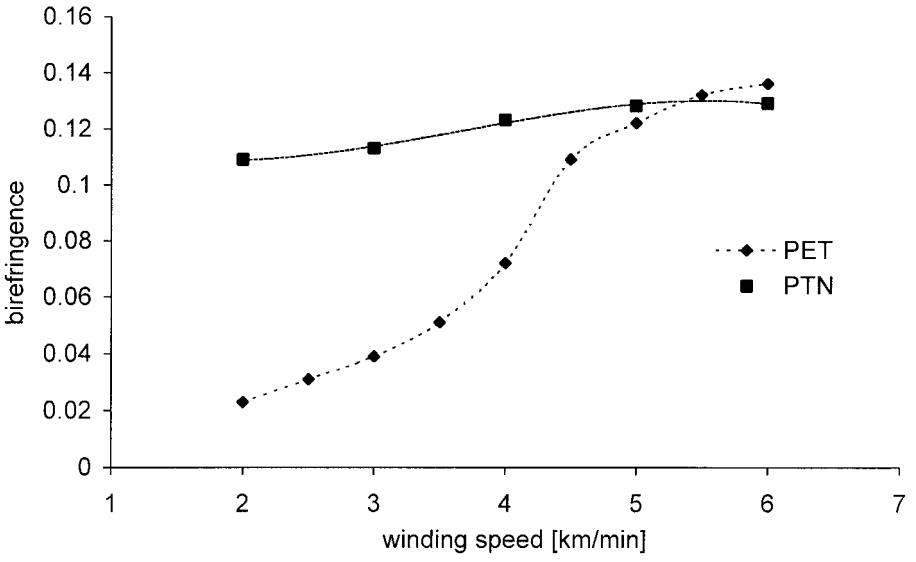

Figure 3 Birefringence as a function of winding speed for PET and PTN fibers.

under isotropic conditions. On the other hand, we observed a marked increase in density from approximately 1.316 to 1.340 g/cm^3 on annealing a PTN fiber above its glass-transition temperature (83°C). Considering these extreme data, it became clear that the density of the as-spun PTN fibers were much closer to ρ_a than to the density of an annealed fiber. Furthermore, we have to remember that ρ_a was determined for the unoriented amorphous state. The density of an oriented amorphous fiber could be somewhat higher than 1.305 g/cm^3 because the chains may be packed in a more compact manner. Therefore, we can conclude that the as-spun PTN fibers were either fully amorphous or contained a fairly low fraction of crystalline material. To get more information, X-ray experiments were carried out (c.f. next discussion).

A relative estimate of molecular orientation could be obtained with the birefringence of a maximum oriented fiber as the reference point. For a fully drawn PTN fiber, the birefringence was 0.204. The birefringence of the as-spun PTN fibers reached only approximately 65% of this value even at a high winding speed.

Calorimetric Analysis

Figure 4 shows the DSC heating traces as a function of winding speed for as-spun PET and PTN fibers. The heating traces of a PET fiber exhibited a crystallization exotherm between 2000 and 5000 m/min as a result of thermally induced crystallization taking place during the DSC heating process. The magnitude of the crystallization peak decreased significantly with increasing take-up velocity due to a rising level of well-developed crystalline structures forming already during the spinning process.[3] Above 5000 m/min, the crystallization peak vanished entirely as spin-crystallization came to completion. The melting peak also shifted from 258 to 270°C with the beginning of spin-crystallization. The higher melting peak temperature could be correlated with the presence of larger crystallites in the as-spun PET fiber.

Unlike the PET fiber, the melting peak temperature of an as-spun PTN fiber was nearly independent of winding speed at 207°C. As there is a correlation between melting peak temperature and crystallite size, we could conclude that even under high spinning stress, the crystallite size did not rise significantly. Moreover, the heating traces of fibers obtained over the whole range of winding speeds studied showed a crystallization exotherm. This means that the crystallinity achieved during the spinning process was much lower than what was attainable, even when high spinning stress was applied.

The magnitude of the melting enthalpy (ΔH_m) is another measure of crystallinity. Because we were interested in the crystallinity of the as-spun fibers, the postcrystallization during the DSC run obscured the results, and its effect had to be eliminated. This was done by consideration of the real

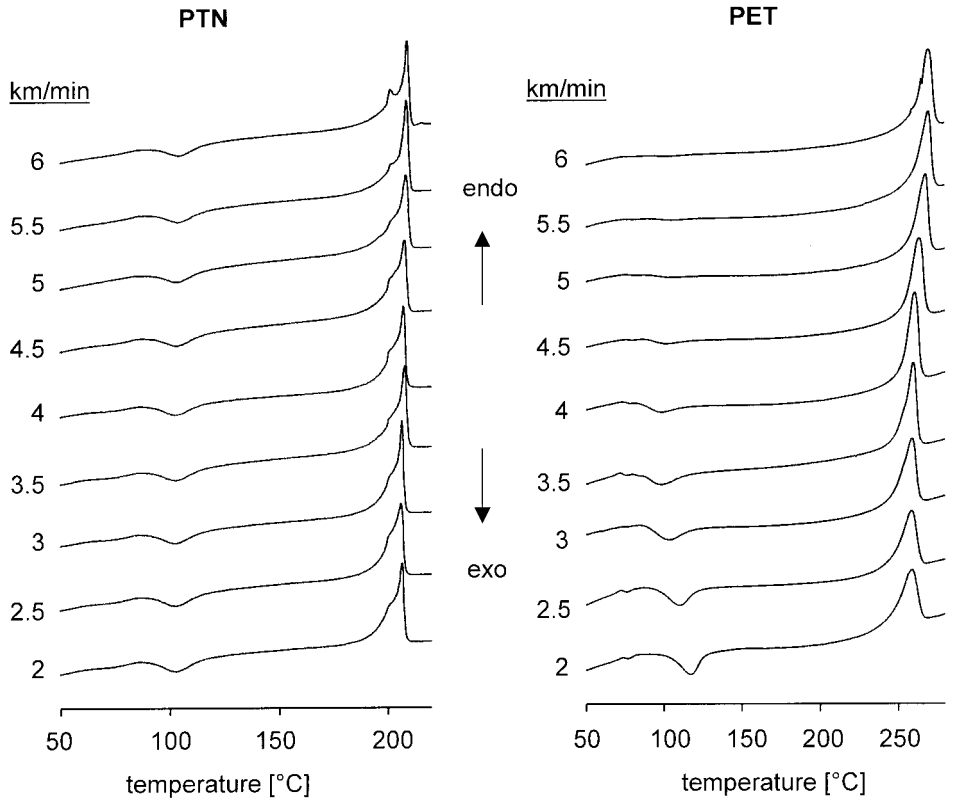

Figure 4 DSC heating traces as a function of winding speed for PET and PTN fibers.

melting enthalpy, $\Delta H'_m$, of a fiber, obtained by the addition of the crystallization enthalpy ΔH_c (negative) and ΔH_m (positive) according to eq. (1):

$$\Delta H'_m = \Delta H_m + \Delta H_c \quad (1)$$

Some caution is necessary, however, when discussing the enthalpy values in terms of crystallinity. It is neglected that ΔH_m depends on the crystallite size. At the melting point, the phase boundary between crystalline and noncrystalline phases disappears. The smaller the crystallites are, the more the resulting surface energy reduces ΔH_m. Furthermore, eq. (1) assumes that the standard enthalpies of crystallization and melting are the same.

According to Figure 5, $\Delta H'_m$ of a PET fiber spun at 2000 m/min was approximately 25 J/g. As the DSC records the melting of the crystalline phase a PET fiber spun below the critical take-up velocity of approximately 3500 m/min should ideally show a $\Delta H'_m$ of zero. Furthermore, the beginning of stress-induced crystallization was not clearly indicated at 3500 m/min. To summarize, a quantitative conclusion about the amount of crystallinity could not be obtained from the calorimetric analysis, especially for PET fibers spun at a low speed.

In the case of PTN fibers, $\Delta H'_m$'s were nearly independent of winding speed. This means that a higher spinning stress had only a small influence on crystallinity, which is in agreement with our density measurements discussed previously. The fact that the crystallite size was independent of winding speed let us assume that $\Delta H'_m$'s in Figure 5 should indicate correctly the relative change in crystallinity.

X-Ray Analysis

Figure 6 shows the WAXS pattern of a PTN fiber spun at 2000 m/min. As a consequence of the orientation of the molecules in the noncrystalline phase, the WAXS pattern exhibited an amorphous halo showing an uneven intensity distribution with a greater intensity on the equator. Some clear crystallite reflections were also present. They were due to stress-induced crystallization during melt spinning at 2000 m/min. Obviously, a small spinning stress ($<$ 2000 m/min) was sufficient to generate a two-phase structure of crystal-

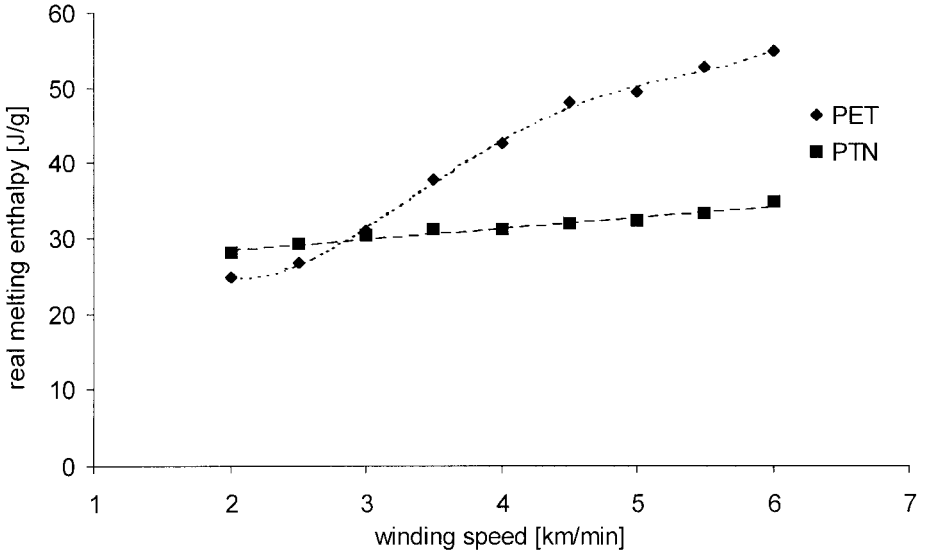

Figure 5 $\Delta H'_m$ as a function of winding speed for PET and PTN fibers.

line and noncrystalline domains in an as-spun PTN fiber. In contrast, stress-induced crystallization in a PET fiber was only observed above 3500 m/min.[1,3]

Boiling Water Shrinkage

Figure 7 shows the boiling water shrinkage as a function of winding speed for as-spun PET and PTN fibers. Such shrinkage can occur because, in boiling water, the glass-transition temperature is exceeded and the macromolecules in the noncrystalline phase possibly have sufficient mobility to attain their most probable conformation. As a well-oriented macromolecule is in a low-entropy conformation, it has a pronounced tendency to relax and coil up.

In semicrystalline polymeric material, the crystallites act essentially as crosslinks. They are interconnected and fixed in space via tie molecules. This rigid supermolecular structure can prevent a coil-up of oriented macromolecules in the noncrystalline domains; hence, the shrinkage is largely reduced if crystallites are present.

The thermal shrinkage of an as-spun PET fiber decreased dramatically as the winding speed exceeded 3000 m/min due to an increasing number of crystallites. Above 4500 m/min, the number of crystallites acting as crosslinks was so high that shrinkage did not occur to an appreciable extent.

Unlike the PET fiber, the as-spun PTN fiber revealed a constant shrinkage over all winding speeds. The low shrinkage of approximately 14% could be attributed to the presence of crystallites that were formed as a consequence of stress-induced crystallization. The fact that the shrinkage was constant supports the view that the crystallinity is fairly independent of winding speed.

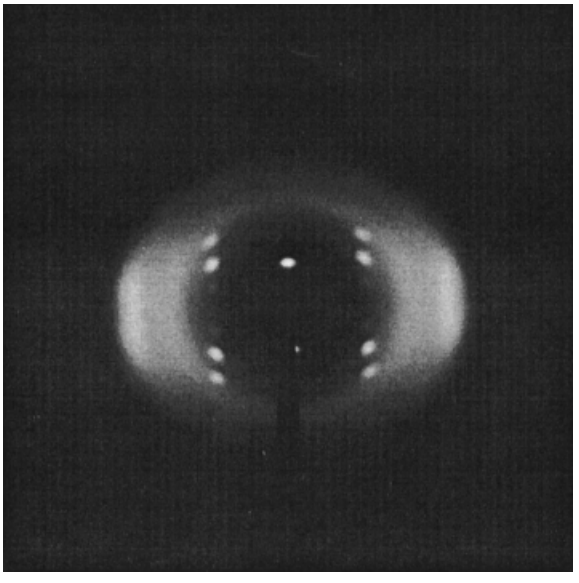

Figure 6 WAXS pattern of a PTN fiber spun at 2000 m/min.

Tensile Properties

Figures 8 and 9 show tenacity and elongation at break as a function of winding speed for as-spun PET and PTN fibers. The tenacity of the PET

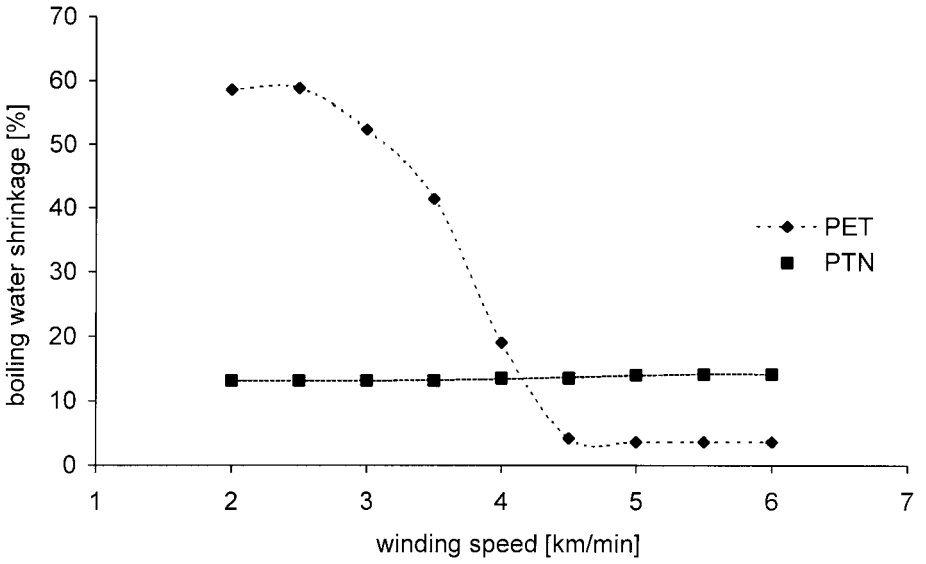

Figure 7 Boiling water shrinkage as a function of winding speed for PET and PTN fibers.

fibers increased in a steady linear fashion from 18 to 36 cN/tex when the winding speed was raised from 2000 to 6000 m/min, whereas the elongation at break decreased exponentially from 180 to 60%. For the as-spun PTN-fibers, the effect of winding speed was markedly smaller, with tenacity increasing only from 21 to 26 cN/tex and the elongation at break decreasing from 60 to 30%. Figure 10 shows the modulus as a function of winding speed for as-spun PET and PTN fibers. Similar to tenacity, the modulus of an as-spun PET fiber increased steadily from 16 to 66 cN/dtex, whereas the modulus of an as-spun PTN fiber increased only slightly from 21 to 26 cN/dtex.

As the modulus of a PET crystal is approximately an order of magnitude greater than the modulus of any PET filament ever produced, it is widely accepted that the strength and modulus depend on the structure of the amorphous phase.[1–4] Consequently, the number and distribution of length of tie molecules in semicrystal-

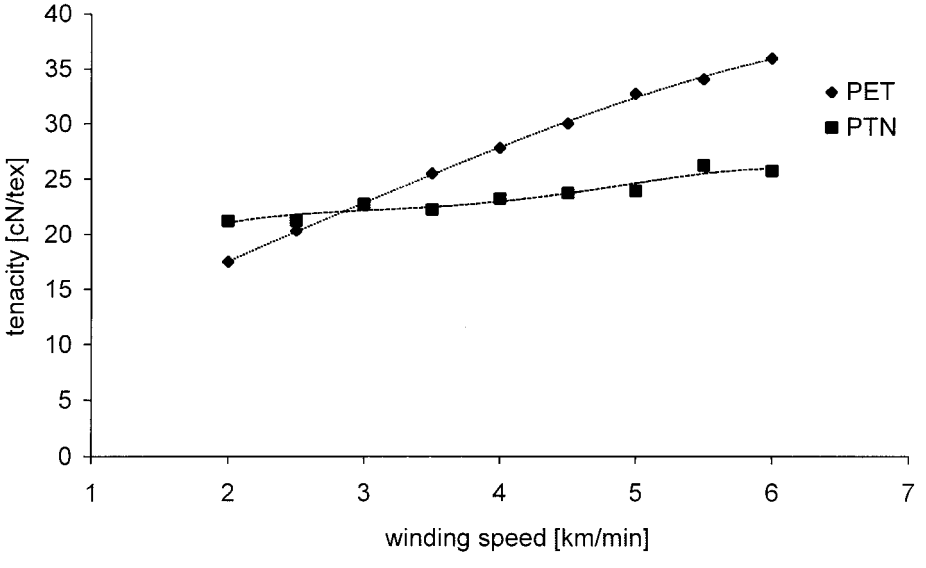

Figure 8 Tenacity as a function of winding speed for PET and PTN fibers.

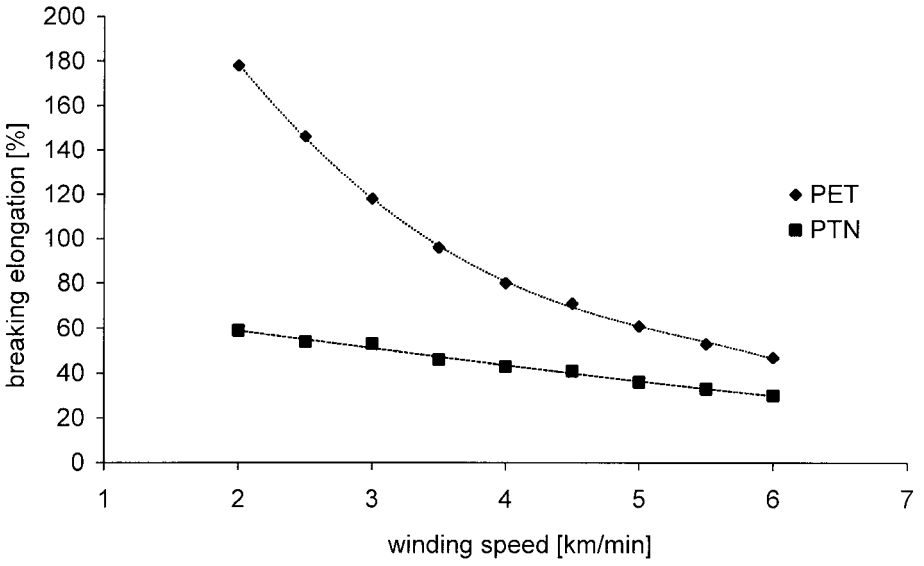

Figure 9 Breaking elongation as a function of winding speed for PET and PTN fibers.

line polymeric material will control to a great extent the mechanical behavior of filaments.

We could show that the use of higher winding speeds did not induce significant structural change in as-spun PTN fibers. Thus, the fact that tenacity, elongation at break, and modulus did not change significantly was due to these low structural changes. Because the stress-induced crystallization of an as-spun PTN fiber took place below 2000 m/min, the crosslinks led to a higher modulus between 2000 and 3000 m/min, as compared to that of a PET fiber. Above approximately 3500 m/min, where the stress-induced crystallization of the as-spun PET fiber set in, the modulus of the PET fiber increased rapidly due to a higher number of effective crosslinks.

CONCLUSIONS

We have shown that the two polymer materials PET and PTN exhibited remarkably different behavior during melt spinning. PET remained essentially amorphous when the winding speed did

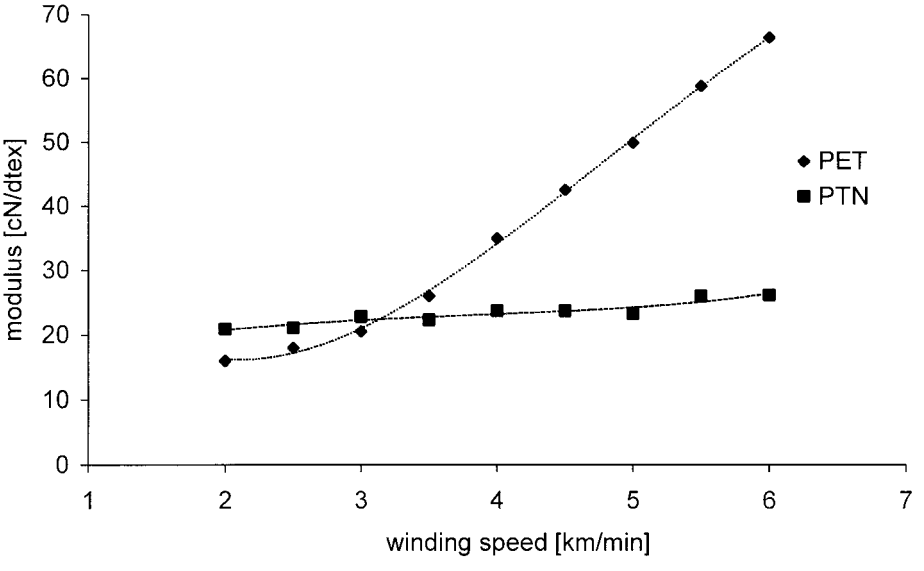

Figure 10 Modulus as a function of winding speed for PET and PTN fibers.

not exceed approximately 3000 m/min. At higher winding speeds, stress-induced crystallization appeared rather abruptly, with the crystallinity rising in a narrow window of winding speeds. Concurrently, the boiling water shrinkage was markedly reduced.

With PTN, on the other hand, the small stress generated at the lowest winding speed studied (2000 m/min) was sufficient to induce some crystallinity. This was easily detected by WAXS. An increase of winding speed up to 6000 m/min only resulted in a minor enhancement of crystallinity. The molecular orientation monitored by birefringence also did not change appreciably. Thermal analysis showed that in all of the as-spun fibers, the crystallinity could be increased noticeably by annealing.

These observations led to the following picture of fiber formation with PTN. The small fraction of crystallites formed even at low winding speeds was stabilizing the morphology to such an extent that it was not possible to further increase the orientation. This, in turn, means that the crystallinity remained constant at a low level with rising winding speed, and the macroscopic tensile properties showed only slight enhancement.

REFERENCES

1. Lim, J. Y.; Kim, S. Y. J Appl Polym Sci 1999, 71, 1283.
2. Fu, Y.; Annis, B.; Boller, A.; Jin, Y.; Wunderlich, B. J Polym Sci Part B: Polym Phys, 32, 2289.
3. Hotter, J. F.; Cuculo, J. A.; Tucker, P. A.; Annis, B. K. J Appl Polym Sci 1998, 69, 2115.
4. Murase, S.; Kudo, K.; Hirami, M. J Appl Polym Symp 1995, 47, 161.
5. Huisman, R.; Heuvel, H. M. J Appl Polym Sci 1989, 37, 595.
6. Falkei, B.; Giessler, W.; Schultze-Gebhardt, F.; Spilgies, G. Angew Makromol Chem 1982, 108, 9.
7. Heuvel, H. M.; Huisman, R. J Appl Polym Sci 1978, 22, 2229.
8. Huisman, R.; Heuvel, H. M. J Appl Polym Sci 1989, 37, 595.
9. Sharama, V.; Desai, P.; Abhiraman, A. S. J Appl Polym Sci 1997, 65, 2603.
10. Jager, J.; Juijn, J. A.; van den d. Heuvel, C. J. M.; Huijts, R. A. J Appl Polym Sci 1995, 57, 1429.
11. Sharma, N. D.; Jain, S. L. Man-Made Textiles India 1995, 38(10), 406.
12. Rim, P. Chem Fibers Int 1996, 46, 204.
13. Sadanobu, J.; Tsukioka, M. Annu Tech Conf Soc Plast Eng 1997, 55(2), 1567.
14. Hwang, S. K.; Yeh, C.; Chen, L. S.; Way, T. F.; Tsay, L. M.; Liu, K. K.; Chen, L. T. Polym Prepr 1999, 40, 611.
15. How, C.; Forschner, T.; Lowtan, R.; Gwyn, D.; Cristea, B. J Plast Film Sheeting 1999, 15(3), 219.
16. Tsai, R. S.; Lee, Y. D. J Polym Res 1998, 5(2), 77.
17. Stier, U.; Gähr, F; Oppermann, W. J Appl Polym Sci 2001, 80, 2039.
18. Stier, U.; Oppermann, W. J Polym Sci Part A: Polym Chem 2001, 39, 620.
19. Stier, U.; Schawaller, D.; Oppermann, W. Polymer 2001, 42, 8753.
20. Jakeways, R.; Ward, I. M.; Wilding, M. A.; Hall, I. H.; Desborough, I. J.; Pass, M. G. J Polym Sci Polym Phys Ed 1975, 13, 799.
21. Ward, I. M.; Wilding, M. A.; Brody, H. J Polym Sci Polym Phys Ed 1976, 14, 263.
22. Chuah, H. Chem Fibers Int 1996, 46, 426.
23. Traub, H. L.; Hirt, P.; Herlinger, H. Chem Fibers Int 1995, 45, 110.
24. Oppermann, W.; Hirt, P.; Fritz, C.; Chem Fibers Int 1999, 49, 14.